Journal of Oceanology and Limnology
Vol. 36 No. 5, P. 1597-1603, 2018
https://doi.org/10.1007/s00343-018-7004-1

Remote sensing analysis of mangrove distribution and dynamics in Zhanjiang from 1991 to 2011*

LIU Dazhao (刘大召)[1], LI Shanshan (李姗姗)[2], FU Dongyang (付东洋)[1], SHEN Chunyan (沈春燕)[1, **]

[1] *Guangdong Ocean University, Zhanjiang 524088, China*

[2] *School of Tourism and Geographical Sciences, Guangdong University of Finance & Economics, Guangzhou 510320, China*

Received Feb. 19, 2017; accepted in principle Apr. 11, 2017; accepted for publication Aug. 1, 2017

Abstract Mangrove forests provide valuable societal and ecological services and goods. However, they have been experiencing high annual rates of loss in many parts of the world. In order to evaluate a long-term wetland conservation strategy that compromises urban development with comprehensive wetland ecosystem management, remote sensing techniques were used to analyze the changing mangrove distribution in the Zhanjiang Mangrove Forest National Nature Reserve. Between 1991 and 2000, the mangrove area within the study region declined from 2 264.9 to 2 085.9 ha consistent with an annual decrease of 0.79%. However, there was an overall 34.3% increase in mangrove coverage from 2 085.9 to 2 801.8 ha between 2000 and 2011. Major causes of forest loss include local human pressures in the form of deforestation, conversion to agriculture, and natural forces such as erosion. The recent gain in mangrove forest cover is attributed to effective conservation management in the nature reserve area, including intensive mangrove plantation efforts and increased local awareness of wetland conservation.

Keyword: mangrove; landsat TM/ETM+; HJ-1A; conservation; remote sensing

1 INTRODUCTION

Mangrove forests act as habitats and nursery grounds for a wide diversity of marine fauna, and many mangroves are commercially important (Alongi, 2002; Glaser, 2003). Additionally, the current bio-shield function of mangroves is likely to assume greater importance as sea levels rise this century (Alongi, 2008; Carney et al., 2014). Recent research has deemed that mangroves are one of the best geo-indicators of global coastal change research and that their assessment is an excellent method for detecting and quantifying coastal modifications (Souza Filho et al., 2006)

Despite their ecological and socio-economic values, these mangrove forests are declining at an alarming rate (Giri et al., 2007). Decreases in the coverage of mangrove wetlands not only lead to the direct loss of ecological functions along the coastal zone, but also the destruction of natural habitat, which may, for example, threaten the species diversity (Li et al., 2008). While the rates and ultimate causes of such changes have not yet been fully characterized, the remaining mangrove forests are under immense pressure from both natural process such as coastal erosion and anthropogenic factors such as conversion to other land cover (Giri et al., 2007; Satyanarayana et al., 2011; Porwal et al., 2012; Cornforth et al., 2013; Giri et al., 2015; Kanniah et al., 2015).

Conventional monitoring and surveying practices based on field investigations are time-consuming, costly, and labor-intensive for mangrove wetlands partly owing to the marshy nature of their soil and their vast swamps that make mangroves extremely difficult to enter and fully explore. In addition, the appropriate historic field investigation data is not always available, which complicates the performance

* Supported by the National Natural Science Foundation of China (No. 41340049), the Guangdong Province Science and Technology Plan Project (No. 2016A020222016), the Innovation and Strong School Project of Guangdong Ocean University (No. Q16147), and the Natural Science Foundation of Guangdong Province (No. 2016A030313754)

** Corresponding author: cyshen101@163.com

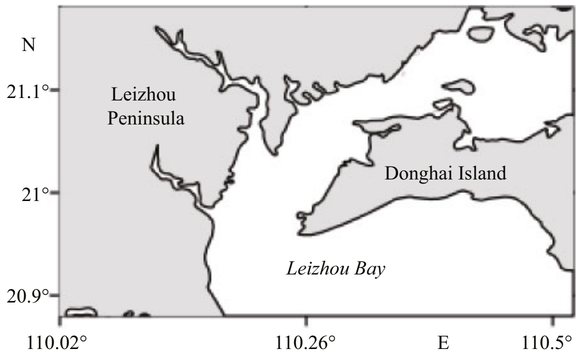

Fig.1 Location map of study area

of time series analysis to investigate changes in mangrove wetlands.

However, rapid progress in remote sensing technology has brought land cover change detection and research into a new era. Remote sensing is poised to play an increasingly important and effective role in the assessment and monitoring of mangrove forest cover dynamics, and the use of remote sensing data offers many advantages, including synoptic coverage, and the availability of low-cost or free satellite data, availability of historical satellite data (Giri et al., 2007).

Several studies have generated maps of mangroves at regional to global levels (Seto and Fragkias, 2007; Li et al., 2008; Giri et al., 2011; Shapiro et al., 2013; Kanniah et al., 2015; Jones et al., 2016). Some researchers have also previously analyzed mangrove forest cover change using satellite data (Giri et al., 2007; Lee and Yeh, 2009; Li et al., 2013; Nascimento et al., 2013; Carney et al., 2014; Giri et al., 2015). Researchers have begun to use high-resolution satellite images (<10 m scale) like Geoeye, Quickbird, or IKONOS datasets to produce more detailed information about mangrove wetlands (Wang et al., 2004; Kovacs et al., 2005; Proisy et al., 2007; Satapathy et al., 2007). Remote sensing analysis of mangroves will increase the transparency of the effects of decision-making (Seto and Fragkias, 2007). In general, remote sensing may therefore become a powerful tool in the assessment and monitoring of mangrove forest cover dynamics (Giri et al., 2007).

The total area of China's mangroves is 22 024.9 ha in 2003, among which Guangdong province accounts for 9 084 ha, or 41% of the total mangroves of China (Li, 2013). Notably, 80% of the mangroves of Guangdong Province are located in Zhanjiang city (Li et al., 2013). The Zhanjiang Mangrove Forest National Nature Reserve was thus established to preserve the valuable remaining mangroves in 1997, and the mangroves have expanded to some extent within the protected areas since then. However, a holistic view of the Zhanjiang Mangrove Forest National Nature Reserve through multi-temporal remote sensing images was not previously available. Changes in mangroves are of critical importance to the region, as these habitats are experiencing increasing threats from coastal development, climate change, and natural disasters (Giri et al., 2015).

In this study, we propose a remote sensing-based approach to determine the extent and location of mangrove forests in the Zhanjiang Mangrove Forest National Nature Reserve in the years 1991, 2000, and 2011. This enabled the quantification and characterization of change dynamics from 1991 to 2011. Using images from two Landsat datasets and one HJ-1A dataset spanning over 20 years, we were able to determine the total mangrove distribution and change.

2 STUDY AREA

The study area is a typical mangrove wetland within the Zhanjiang Mangrove Forest National Nature Reserve that lies in the central eastern portion of the Leizhou Peninsula (Fig.1), which is the largest and the most concentrated area of mangrove wetland in mainland China historically. There are 13 mangrove species in the study area (Gao et al., 2009). The average annual temperature is 22.3°C, with the coolest and warmest weather usually occurring in January and July, respectively (Han and Gao, 2009). The region is also subject to the irregular semi-diurnal tidal regime of the South China Sea (Li et al., 2008). Runoff varies with the seasons, with more than 87% of the total rainfall occurring in the flood season from April to October (Han and Gao, 2009).

3 DATA AND METHOD

The remote sensing data used for mapping and detecting changes in mangroves spanned the period from 1991 to 2011. Pre-processing of remote sensing data such as calibration and atmospheric corrections were performed using ENVI 5.0 software, which included on-site investigations and classification of the remote sensing data.

3.1 Analysis of imagery data

One Landsat Thematic Mapper (TM) image, one Enhanced Thematic Mapper (ETM) image, one HJ-1A image, one digital aerial photograph, one set of

1:10 000-scale topographical maps, and tide level records were used to interpret the locations of mangrove. Both TM and ETM images with 30-m spatial resolutions and HJ-1A images with 28.5-m spatial resolutions were utilized to compare the spatial variation of mangrove forests at different times. The digital aerial photograph with a 0.5-m spatial resolution was used as a reference to assess accuracy. The study area is subject to a humid tropical climate, so cloud coverage often interferes with remote-sensing image acquisition. Thus, there were only few cloud-free images available. Short acquisition date intervals were unfavorable for mangrove change detection, ultimately leaving one TM image from 1991, one ETM image from 2000, and one HJ-1A image from 2011 that were selected for detecting mangrove changes.

All of the image were processed with ENVI5.0. Each image was georeferenced to a topographical map using 46 ground control points (GCP) distributed evenly throughout the study area, which decreased the root mean square error to just 0.5 pixels. The spatial resolution of the HJ-1A data was re-sampled to a 30-m scale in order to make it consistent with the TM and ETM+ data. For this study, atmospheric corrections and calibration to the surface reflectance was conducted using FLAASH (Fast line-of-sight Atmospheric Analysis of Spectral Hypercubes) modules as implemented in ENVI 5.0. We extracted corresponding sub-scene from the three remote sensing images acquired in 1991, 2000, and 2011 in order to match the study area, thus enabling the analysis of changes in the mangrove forest across the different periods.

3.2 In-situ investigation

From 2009 to 2012, we conducted five on-site investigations in the study area in order to obtain information about the mangroves, during which we used global positioning systems to identify the locations of mangrove patches. For each mangrove patch, we determined its borders using global positioning receivers, measured its size, and took panchromatic digital photographs with a digital camera from different perspectives. The mangrove species compositions, mangrove canopy sizes, heights of trees according to visual inspection, and the characteristics of other land cover (such as cropland) were also documented. Over the course of on-site investigation, 434 GCP were collected, among which 172 were used to validate the classification of mangroves via remote sensing, while the remaining GCP were used to examine other classes. We also conducted interviews with regional mangrove planners, village leaders, and the government officials overseeing the Zhanjiang Mangrove Forest National Nature Reserve in order to gain additional insight into mangrove development and variation over the past few decade years.

3.3 Image classification

The unsupervised cluster approach has become a very important spatial data mining method because it does not require the training data to be labeled. Owing to the lack of historical mangroves data for the study area, we used unsupervised classification to map the mangrove forest distribution. The Iterative Self-Organizing Data Analysis Techniques Algorithm (ISODATA) unsupervised classification model was applied to create 30 spectral clusters in ENVI 5.0. The change threshold was set to 5%, and the iterations threshold number was set to 20. The classification process was concluded when either the change threshold or the maximum number of iterations had been reached.

The resulting classification was then divided into the actual land cover and land use classes based upon visual interpretation. Aided by a 1:10 000-scale topographical map released in 1998, tidal level records observed at Naozhou Island station from 1991 to 2011, field investigation logs, and the textures, tones or colors of the image, four land use and land cover types for the study area were determined: (1) mangrove, (2) shrimp and/or crab aquafarm, (3) open water, and (4) other land cover types (e.g., cropland, buildings, and roads). Post-classification editing was conducted to remove obvious errors manually.

3.4 Accuracy assessment

We performed qualitative validation of land cover results using high- resolution digital aerial photography obtained in 2011. This study utilized an equalized stratified random sampling method to assess the accuracy of land cover classification by creating a 15-km by 15 km grid with reference points every 1 km. The accuracy of the four predicted cover classifications from the HJ-1A imagery in 2011 was compared to a 2011 digital aerial photograph. Each of the 353 reference points were compared to the predicted classifications to produce an error matrix. The overall accuracy and Kappa coefficient were used to evaluate the classification accuracy assessment.

Table 1 The producer's and user's accuracy for mangrove classification

Mangrovein aerial photograph	Totally classified mangrove	Correctly classified mangrove	User's accuracy(%)	Producer's accuracy (%)	Kappa coefficient	Overall accuracy (%)
98	112	88	79	90	0.87	88

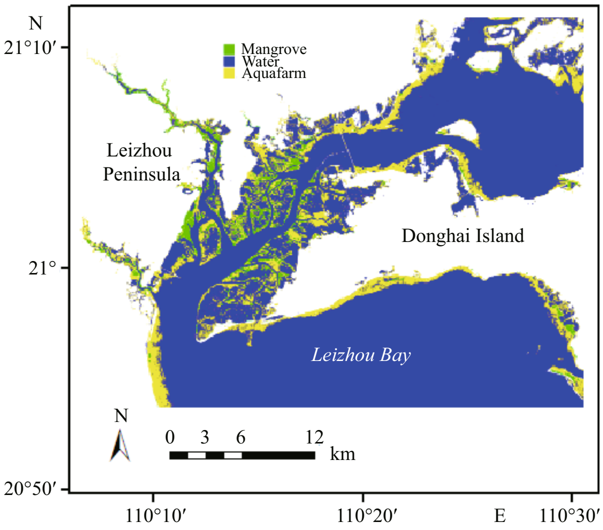

Fig.2 Mangrove coverage in 1991

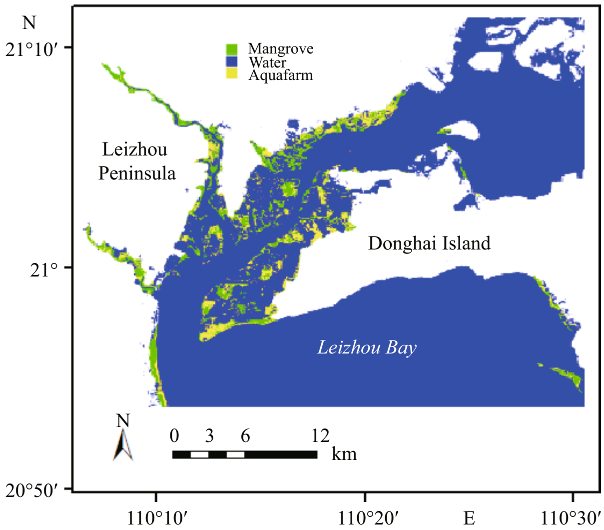

Fig.4 Mangrove coverage in 2011

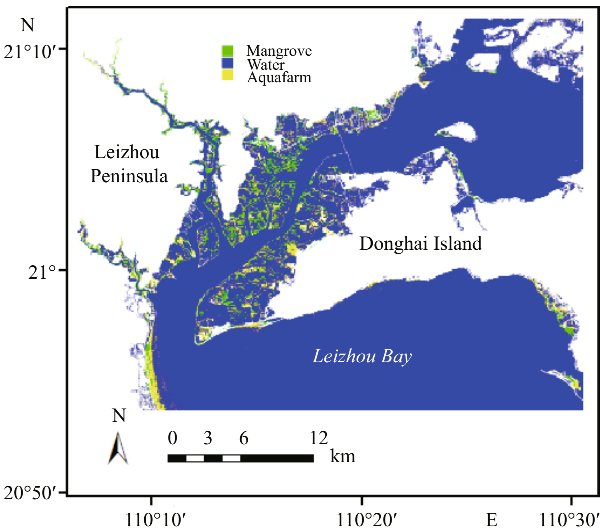

Fig.3 Mangrove coverage in 2000

4 RESULT AND DISCUSSION

4.1 Classification accuracy

The producer's and user's accuracy for mangrove classification was showed in Table 1. The producer's accuracy is 90% and the user's accuracy is 79%, respectively. The totally classified mangrove is predictions from the HJ-1A imagery. An overall accuracy of 88% was achieved for the 2011 classification with a Kappa coefficient of 0.87.

4.2 Mangrove spatial distribution

We retrieved the mangrove wetland distribution maps for 1991, 2000, and 2011 (Figs.2–4). The mangroves mainly distribute along inlet and river estuary of Zhanjiang Bay. Their distribution coincided with the required growth habit of mangroves, specifically warm tidal estuaries. Zhanjiang Bay is encompassed by the mainland and Donghai Island, which together provide adaqute shelter from typhoons for mangrove forests. The satellite imagery analysis for the study area indicated that mangroves covered 2 264.9 ha in 1991, 2 085.9 ha in 2000, and 2 801.8 ha in 2011. Gao et al. (2009) previously estimated that the mangrove area was 2 798.9 ha in 1993 and 1 986.8 ha in 2001, which roughly agrees with our findings.

4.3 Mangrove forest changes

The satellite imagery revealed an overall increase in mangrove coverage, though it also identified sub-regions of stability and loss (Figs.5–6). The largest area of mangrove patch disappearance occurred along the west coast of Zhanjiang Bay over the 1991–2000 period. An interview of the government officials of the Zhanjiang Mangrove Forest National Nature Reserve revealed this area was converted into a shrimp pond. Between 2000 and 2011, the northern and southwestern margins of the mangrove

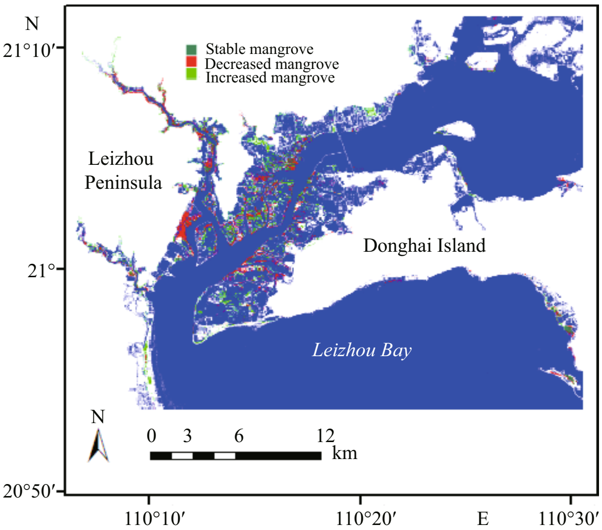

Fig.5 Mangrove forest change from 1991 to 2000

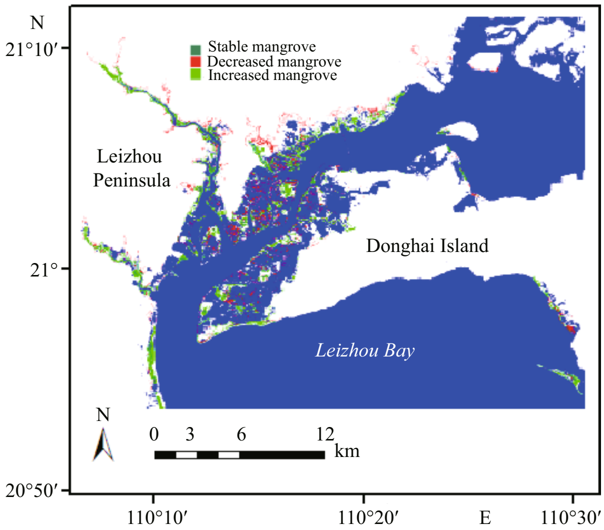

Fig.6 Mangrove forest change from 2000 to 2011

Table 2 Land cover changes from 1991 to 2000 (unit: %)

		2011			
		Mangrove	Aquafarm	Water	Other
1991	Mangrove	30.8	21.9	33.3	14.0
	Aquafarm	5.7	18.7	60.0	15.6
	Water	0.6	2.2	95.5	1.7
	Other	1.5	0.8	1.5	97.3

Table 3 Land cover changes from 2000 to 2011 (unit: %)

		2011			
		Mangrove	Aquafarm	Water	Other
2000	Mangrove	33.5	19.2	28.6	18.7
	Aquafarm	15.5	20.5	41.4	22.5
	Water	1.1	2.6	92.0	4.3
	Other	0.7	1.0	1.4	96.9

Table 4 Land cover changes from 1991 to 2011 (unit: %)

		2011			
		Mangrove	Aquafarm	Water	Other
1991	Mangrove	31.9	20.6	37.7	9.8
	Aquafarm	10.0	13.6	56.3	20.1
	Water	0.8	2.1	93.7	3.4
	Other	0.5	0.7	0.8	98.0

Table 5 Tidal level at image acquisition time

Tidal level (cm)	Date	Data type
218	Oct. 30, 1991	Landsat-5 TM
280	Oct. 30, 2000	Landsat-7 ETM
231	Dec. 25, 2011	Hj-1A

disappeared and the mangrove forest tended to cluster in beachfront areas. More than seven million people live in the urbanized region surrounding the western and southern boundaries of the Zhanjiang Mangrove Forest National Nature Reserve, which has thus exerted substantial human pressure to regional mangroves from harvesting, fishing, and urbanization. Between 1991 and 2000, the increased mangrove patches presented regular shapes. We determined these mangroves were replanted through the field activities. Over this same interval, the mangrove area for the study region declined from 2 264.9 to 2 085.9 ha, representing an annual rate of decrease of 0.79%. However, from 2000 to 2011, there was an overall 34.3% increase in mangrove coverage from 2 085.9 to 2 801.8 ha. We conducted a post-classification change analysis using 1990, 2000, and 2011 mangrove data. Four classification changes were listed in the land cover changes matrix (Tables 2–4). This revealed that from 1991 to 2011, 68.1% of mangrove disappeared, while 10.0% of aquafarm, 0.8% of open water, and 0.5% of other land cover types were converted to mangrove forest. Combined, these represented a total net increase of about 536.9 ha of mangrove cover.

Our analysis indicated that the mangrove forest within the whole study area has been highly dynamic throughout the 1991–2011 periods. There have been simultaneous processes of cumulative forest gain and loss occurring in the region. For example, 69.2% of plots covered by the mangrove forest in 1991 had been transformed into aquafarm, open water, or another land cover types by 2000. However, during the same period, 81.3% of aquafarm had been converted to mangrove, open water, or another land cover type. The turnover for mangrove and aquafarm classes were quite high, with only 30.8% of mangrove and 18.7% of aquafarm areas remaining steadily classified. Similar dynamic patterns were observed in the 2000–2011 and 1991–2011 periods.

As mangroves are always distributed in intertidal zones, they are strongly affected by local tidal rhythms. Indeed, Giri et al. (2007), Li et al. (2008), and Li et al. (2013) have all noted the effects of tidal inundation in their satellite-based mangrove area estimates. Comparisons between the classification images of 1991 and 2011 revealed that the mangrove and aquafarm patches surrounded by water were obviously most fragmented in 2000. Moreover 33.3% of mangrove and 60% of aquafarm areas were converted to open water from 1991 to 2000 as shown in Table 3.

The acquisition times of the three image were the same. The tidal level at the remote sensing image acquisition time is listed in Table 5. The 2000 tidal level was about 280 cm, which is 62 cm higher than that in 1991. This higher tide level inundated the aquafarm and mangrove areas, especially small mangrove areas, and thus led to an underestimation of the mangrove area as assessed by satellite imagery.

The high turnover rate between aquafarm and open water areas may possibly be a consequence of differing tidal level at the image acquisition time between 1991 and 2000. Tide level fluctuations can easily cause the misclassification of mangrove, aquafarm, and open water from one another. Over the same interval, the mangrove area decreased by 7.9%. Given the much higher tidal levels in 2000 relative to 1991, this decrease may be imprecise. Similarly, the estimated mangrove area increase from 2000 to 2011 was impacted by the lower tidal level of 2011 relative to that of 2000. The tidal level of 2011 was 13 cm higher than that of 1991, while the mangrove area increased by 23.7%, indicating that the estimate is conservative and that the mangrove area increased by at least 23.7% over the previous twenty years.

Satellite-based approaches tend to underestimate mangrove distributions as they are easily affected by local tidal cycles (Li et al., 2013). In order to reveal the actual distribution, it is best to utilize satellite data at the same tidal level across years. However, the dearth of scenes in which images were free of clouds in the study area over the past twenty years limited the useable data. Hence, this is a difficult analysis to conduct. In contrast, airborne remote sensing can effectively obtain such data at times of low tide and low cloud cover. In addition, this approach delivers the added benefit of high spatial resolution. Thus, airborne remote sensing is an efficient alternative for monitoring mangrove changes at a local scale.

The Zhanjiang Mangrove Forest National Nature Reserve was established in 1997. Official government protection has prohibited the harvesting of mangroves for lumber or firewood and thus the mangrove regeneration has been observed within the intertidal zone. The remote sensing data also indicated the mangrove forest increased over the past twenty years at an annual rate of 1.19%. In total, 1 200 ha of mangrove was planted by local communities during 1985−1990 and then another 1 000 ha of plantations were planted by the Sino-Dutch Integrated Mangrove Management and Coastal Protection project during 2001−2007 (Gao et al., 2009).

5 CONCLUSION

In this study, we used multi-temporal satellite data to assess the mangrove area distribution and changes of the Zhanjiang Mangrove Forest National Nature Reserve. The analysis showed that mangrove forests in the Zhanjiang wetlands increased by at least 23.7% from 1991 to 2011. The rate of change was variable over time; between 1991 and 2000, mangrove forest area decreased by 7%, while from 2000 to 2011, the area increased by 34.3%.

Mangrove loss is mainly attributed to deforestation, conversion for agricultural and residential use, and erosion. The increase in mangrove forest cover may be attributed to conservation efforts in the reserve area, such as intensive mangrove plantation efforts and greater local and national awareness of the importance of wetland conservation. Despite natural losses and human pressures, mangroves increased by 536.9 ha from 1991 to 2011.

The Zhanjiang mangrove wetland is highly dynamic. The high turnover among mangrove, aquafarm, and open water areas may be a result of tidal fluctuations. Satellite-based approaches tend to underestimate mangrove distributions. As these methods are clearly affected by local tidal cycles, airborne remote sensing is an efficient alternative for monitoring mangrove changes at a local scale.

6 DATA AVAILABILITY STATEMENT

The TM and ETM dataset that support the findings of this study are available in https://landsat.usgs.gov/landsat-data-access, and the HJ-1A data that support the findings of this study are available in http://www.cresda.com/CN/.

7 ACKNOWLEDGEMENT

We also thank many colleagues from Guangdong Ocean University for their hard-work on in-situ investigation. We would also like to express our gratitude to anonymous reviewers.

References

Alongi D M. 2002. Present state and future of the world's mangrove forests. *Environ. Conserv.*, **29**(3): 331-349.

Alongi D M. 2008. Mangrove forests: resilience, protection from tsunamis, and responses to global climate change. *Estuarine Coastal Shelf Sci.*, **76**(1): 1-13.

Carney J, Gillespie T W, Rosomoff R. 2014. Assessing forest change in a priority West African mangrove ecosystem: 1986-2010. *Geoforum*, **53**: 126-135.

Cornforth W A, Fatoyinbo T E, Freemantle T P et al. 2013. Advanced land observing satellite phased array type L-Band SAR (ALOS PALSAR) to inform the conservation of mangroves: Sundarbans as a case study. *Remote Sens.*, **5**(1): 224-237.

Gao X M, Han W D, Liu S Q. 2009. The mangrove and its conservation in Leizhou Peninsula, China. *J. Fores. Res.*, **20**(2): 174-178.

Giri C, Long J, Abbas S et al. 2015. Distribution and dynamics of mangrove forests of South Asia. *J. Environ. Manage.*, **148**: 101-111.

Giri C, Ochieng E, Tieszen L L et al. 2011. Status and distribution of mangrove forests of the world using earth observation satellite data. *Global Ecol. Biogeogr.*, **20**(1): 154-159.

Giri C, Pengra B, Zhu Z L et al. 2007. Monitoring mangrove forest dynamics of the Sundarbans in Bangladesh and India using multi-temporal satellite data from 1973 to 2000. *Estuarine Coastal Shelf Sci.*, **73**(1-2): 91-100.

Glaser M. 2003. Interrelations between mangrove ecosystem, local economy and social sustainability in Caeté Estuary, North Brazil. *Wetlands Ecol. Manage.*, **11**(4): 265-272.

Han W D, Gao X M. 2009. The Mangrove Ecosystem and Its Conservation Strategy in Leizhou Peninsula. South China University of Technology Press, Guangzhou, China. (in Chinese)

Jones T G, Glass L, Gandhi S et al. 2016. Madagascar's mangroves: quantifying nation-wide and ecosystem specific dynamics, and detailed contemporary mapping of distinct ecosystems. *Remote Sens.*, **8**(2): 106.

Kanniah K D, Sheikhi A, Cracknell A P et al. 2015. Satellite images for monitoring mangrove cover changes in a fast growing economic region in southern peninsular Malaysia. *Remote Sens.*, **7**(11): 14 360-14 385.

Kovacs J M, Wang J F, Flores-Verdugo F. 2005. Mapping mangrove leaf area index at the species level using IKONOS and LAI-2000 sensors for the Agua Brava Lagoon, Mexican Pacific. *Estuarine Coastal Shelf Sci.*, **62**(1-2): 377-384.

Lee T M, Yeh H C. 2009. Applying remote sensing techniques to monitor shifting wetland vegetation: a case study of Danshui River estuary mangrove communities, Taiwan. *Ecol. Eng.*, 3**5**(4): 487-496.

Li C G. 2013. Research on Remote Sensing Information Extraction and the Evolution Mechanism of Mangrove. Science Press, Beijing, China. (in Chinese)

Li M S, Mao L J, Shen W J et al. 2013. Change and fragmentation trends of Zhanjiang mangrove forests in southern China using multi-temporal Landsat imagery (1977-2010). *Estuarine Coastal Shelf Sci.*, **130**: 111-120.

Li T H, Han P, Zhao Z J. 2008. Impact Analysis of coastal engineering projects on mangrove wetland area change with remote sensing. *China Ocean Eng.*, **22**(2): 347-358.

Nascimento W R Jr, Souza-Filho P W M, Proisy C et al. 2013. Mapping changes in the largest continuous Amazonian mangrove belt using object-based classification of multisensor satellite imagery. *Estuarine Coastal Shelf Sci.*, **117**: 83-93.

Porwal M C, Padalia H, Roy P S. 2012. Impact of tsunami on the forest and biodiversity richness in Nicobar Islands (Andaman and Nicobar Islands), India. *Biodivers. Conserv.*, **21**(5): 1 267-1 287.

Proisy C, Couteron P, Fromard F. 2007. Predicting and mapping mangrove biomass from canopy grain analysis using Fourier-based textural ordination of IKONOS images. *Remote Sens. Environ.*, **109**(3): 379-392.

Satapathy D R, Krupadam R J, Kumar L P et al. 2007. The application of satellite data for the quantification of mangrove loss and coastal management in the Godavari estuary, East Coast of India. *Environ. Monit. Assess.*, **134**(1-3): 453-469.

Satyanarayana B, Koedam N, De Smet K et al. 2011. Long-term mangrove forest development in Sri Lanka: early predictions evaluated against outcomes using VHR remote sensing and VHR ground-truth data. *Mar. Ecol. Prog. Ser.*, **443**: 51-63.

Seto K C, Fragkias M. 2007. Mangrove conversion and aquaculture development in Vietnam: a remote sensing-based approach for evaluating the Ramsar Convention on Wetlands. *Global Environ. Change*, **17**(3-4): 486-500.

Shapiro A C, Trettin C C, Küchly H, Alavinapanah S, Bandeira S. 2013. The mangroves of the Zambezi delta: increase in extent observed via satellite from 1994 to 2013. *Remote Sens.*, **7**(12): 16 504-16 518.

Souza Filho P W M, Farias Martins E D S, Da Costa F R. 2006. Using mangroves as a geological indicator of coastal changes in the Bragança macrotidal flat, Brazilian Amazon: a remote sensing data approach. *Ocean Coastal Manage.*, **49**(7-8): 462-475.

Wang L, Sousa W P, Gong P et al. 2004. Comparison of IKONOS and QuickBird images for mapping mangrove species on the Caribbean coast of Panama. *Remote Sens. Environ.*, **91**(3-4): 432-440.